

Resolving mutually-coherent point sources of light with arbitrary statistics

Ilya Karuseichyk ^{*}, Giacomo Sorelli , Mattia Walschaers , and Nicolas Treps

Laboratoire Kastler Brossel, Sorbonne Université, CNRS, ENS-Université PSL, Collège de France, 4 place Jussieu, F-75252 Paris, France

Manuel Gessner

*ICFO-Institut de Ciències Fotòniques, The Barcelona Institute of Science and Technology,
Av. Carl Friedrich Gauss 3, 08860, Castelldefels (Barcelona), Spain*

and Departamento de Física Teórica and IFIC, Universidad de Valencia-CSIC, C/ Dr. Moliner 50, 46100 Burjassot (Valencia), Spain



(Received 13 April 2022; accepted 31 August 2022; published 7 October 2022)

We analyze the problem of resolving two mutually coherent point sources with arbitrary quantum statistics, mutual phase, and relative and absolute intensity. We use a sensitivity measure based on the method of moments and compare direct imaging with spatial-mode demultiplexing (SPADE), analytically proving advantage of the latter. We show that the moment-based sensitivity of SPADE saturates the quantum Fisher information for all known cases, even for non-Gaussian states of the sources.

DOI: [10.1103/PhysRevResearch.4.043010](https://doi.org/10.1103/PhysRevResearch.4.043010)

I. INTRODUCTION

The problem of resolving two point sources has been intensively studied as a model problem for optical system resolution characterization for more than a century. For a long time, only visual observation of the light coming from the sources was available; thus, resolving criteria, such as Rayleigh criterion, were based on characteristics of intensity distribution resolvable by the human eye [1,2]. However, it is possible to resolve sources beyond visual resolution criteria by performing a full statistical analysis of the intensity distribution in the image plane [3]. One can estimate the separation of the two sources from this measurement, and the efficiency of this estimation can be evaluated based on the Cramér-Rao bound, which is expressed in terms of the Fisher information (FI). We refer to spatially resolved intensity measurements as direct imaging (DI). This technique often leads to a vanishing FI in the limit of small separations; this feature, known as *Rayleigh's curse* [4], implies that a larger number of measurements is needed to resolve smaller separations. At the same time, an analysis of the quantum FI (QFI), which provides the ultimate resolution limit, showed that, in most cases, one can increase the resolution and avoid Rayleigh's curse by choosing a better measurement than DI [4].

A good example of such a measurement is spatial-mode demultiplexing (SPADE) [4,5]. SPADE proposes to decompose the field in the image plane into spatial modes and to measure the intensity in each of these modes. With the

appropriate choice of the measurement modes, all the information about the parameters is often encoded into a small number of modes. This allows us to use faster and less noisy detectors than array detectors required for DI. The resolution of SPADE for uncorrelated thermal sources was widely studied theoretically [6–11] and experimentally [12–14]. The FI of this measurement, calculated in the limit of small photon numbers, was proved to saturate the ultimate bound set by the QFI [5,15]. Recently, another measure of resolution was proposed—a sensitivity measure based on the method of moments [16,17]. This measure allowed us to analyze the problem of resolving bright uncorrelated thermal sources and proved SPADE to saturate the ultimate limits without the need to assume low source intensities [8,9]. Moreover, the moment-based approach gives a practical way to determine a bound on the sensitivity of specific measurements which can be saturated by a parameter retrieval method that does not require complicated data processing. Since this method is based only on the mean values of the observables, it can be effectively implemented with slow detectors, not resolving individual pulses.

While early results focused on incoherent sources, the role of the mutual coherence of the sources was the subject of recent discussions [18–25]. Despite these studies, there are still gaps in knowledge in this area. This is especially true for bright sources since most of the cited research is based on the assumption of low intensity of the detected signal. Nevertheless, the study of the QFI of partially correlated thermal light shows a significant influence of the brightness of the sources on resolution limit [15,26]. Thus, for practical application of SPADE, it is important to develop its description for the case of bright sources and to identify a practical estimator for the separation from the measurement results.

In this paper, we focus on the fundamentally and practically important case of a pair of perfectly mutually coherent sources. Within this framework, in contrast to previous works

^{*}ilya.karuseichyk@lkb.upmc.fr

Published by the American Physical Society under the terms of the Creative Commons Attribution 4.0 International license. Further distribution of this work must maintain attribution to the author(s) and the published article's title, journal citation, and DOI.

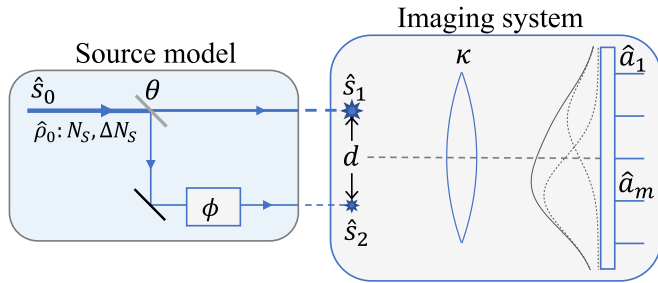


FIG. 1. On the left: conceptual scheme for generating a general two-mode coherent state based on a beam splitter with transmissivity $T = \cos^2 \theta$ and a phase shifting element ϕ . On the right: optical scheme for the estimation of the separation of the sources, where κ is the transmissivity of the imaging system, and photon counting is performed in the measurement modes $f_m(\vec{r})$ with corresponding field operators \hat{a}_m .

[5,7,8,15,21], we consider the most general quantum state of the emitted light and make no assumption about the absolute and relative brightness and relative phase of the sources. Using the method of moments, we analyze the sensitivity of DI and SPADE for the estimation of the separation of the sources. We present an upper bound for the resolution of the DI technique and analytically prove an advantage of the SPADE approach for a wide range of parameters and various quantum states. Considering a multiparameter estimation approach, we analytically find the separation estimation sensitivity with and without prior knowledge about the brightness of the sources. We show that antibunching of the radiation of the sources leads to an increase of the sensitivity, but at the same time, the ignorance of the brightness of the sources wipes out any possible profit from nonclassical statistics of the sources. Finally, we show that the calculated sensitivity saturates the QFI for those cases where it is known. On top of traditional examples of coherent and thermal states, these include non-Gaussian states of the sources such as entangled Fock states, for which the QFI of separation estimation is maximal [15]. Obtained results can be easily generalized to other parameter estimation problems based on photon counting and mutually coherent probes or a single-mode probe, like coherent imaging [27] or even distributed quantum sensing [28].

The outline of the paper is as follows. In Sec. II, we introduce the model of the sources and describe detection of the emitted light. Section III describes the method of moments and presents the sensitivities for the single- and multiparameter cases. In Secs. IV and V, we analyze the sensitivity coming from relative and total intensity measurements, respectively. In Sec. VI, we compare the obtained sensitivity with the QFI.

II. SOURCES AND DETECTION MODELS

We consider an optical scheme for parameter estimation, where two pointlike sources emit light, which passes through a diffraction-limited imaging system (see the right part of Fig. 1). Then the parameters of the sources, such as the separation d , are estimated from measurements of the diffracted light.

A. Emitted field

Point sources emit light in the orthogonal modes with field operators $\hat{s}_{1,2}$. We only consider mutually coherent sources, meaning that the absolute value of the first-order degree of coherence of the emitted light is $|g^{(1)}| = 1$. One can always find a single mode (called the *principal mode*) that fully describes this field configuration. Thus, the most general mutually coherent state of the modes $\hat{s}_{1,2}$ can be considered the result of splitting some mode \hat{s}_0 on an asymmetric beam splitter with transmissivity $T = \cos^2 \theta$ and adding a phase ϕ to one of the output modes $\hat{s}_{1,2}$ (see the left part of Fig. 1). The first-order coherency matrix of the modes $\hat{s}_{1,2}$ reads

$$\langle \hat{s}_j^\dagger \hat{s}_k \rangle = \begin{bmatrix} N_S \cos^2 \theta & \frac{N_S}{2} \sin 2\theta \exp(i\phi) \\ \frac{N_S}{2} \sin 2\theta \exp(-i\phi) & N_S \sin^2 \theta \end{bmatrix}, \quad (1)$$

where $N_S = \text{Tr}(\hat{\rho}_0 \hat{s}_0^\dagger \hat{s}_0)$ is the average number of emitted photons, and the parameter θ is responsible for the asymmetry of source intensities, i.e., the ratio between the brightness of the sources is given by $\langle \hat{s}_2^\dagger \hat{s}_2 \rangle / \langle \hat{s}_1^\dagger \hat{s}_1 \rangle = \tan^2 \theta$. For concreteness, we assume the parameter θ to be within a range $0 \leq \theta \leq \pi/4$, where $\theta = \pi/4$ corresponds to equally bright sources and $\theta = 0$ to all light in mode \hat{s}_1 . The parameter $\gamma = \langle \hat{s}_1^\dagger \hat{s}_2 \rangle / \sqrt{\langle \hat{s}_1^\dagger \hat{s}_1 \rangle \langle \hat{s}_2^\dagger \hat{s}_2 \rangle} = \exp(i\phi)$ is often referred to as the degree of mutual coherence between modes, and in our case, it has modulus equal to one.

Note that no assumptions about state $\hat{\rho}_0$ of the mode \hat{s}_0 was made so far: If it is in the coherent state, then the state of the modes $\hat{s}_{1,2}$ is uncorrelated; for thermal statistics of $\hat{\rho}_0$, the modes $\hat{s}_{1,2}$ are classically correlated; for Fock states of \hat{s}_0 , the output modes are entangled.

For further description of the parameter estimation in terms of the method of moments, we will only need the two first moments for the state $\hat{\rho}_0$: the average photon number N_S and its variance ΔN_S^2 . Thus, a sufficient description of the emitted field is provided by the set of parameters $\{N_S, \Delta N_S, \theta, \phi\}$.

B. Field detection

The emitted light goes through an imaging system with finite aperture that has a transmissivity κ and point spread function (PSF) $u_0(\vec{r})$. Within the paraxial approximation, we can assume that the transmissivity κ does not depend on the positions of the sources. In the image plane, the light is detected either directly (DI) or via SPADE. Both cases can be described as measurement over some field modes $f_m(\vec{r})$ with corresponding operators \hat{a}_m , where for DI, $f_m(\vec{r})$ are localized pixel modes, and for SPADE, $f_m(\vec{r})$ are more general non-localized modes, for example, the Hermite-Gauss modes. Then the parameters of interest are estimated from the measured numbers of photons in the detection modes $N_m = \langle \hat{a}_m^\dagger \hat{a}_m \rangle$. We analyze the estimation of the separation of the sources d with and without prior knowledge of the number of emitted photons N_S .

Passing through the lossy optical system can be described as a mixing of the field modes with vacuum modes [15]. Considering also the vacuum mode from the beam splitter defined by the parameter θ (see Fig. 1), the field operators of the measurement modes can be represented as $\hat{a}_m = A_m \hat{s}_0 + \hat{v}_m$, where A_m are complex coefficients and \hat{v}_m are nonnormalized

nonorthogonal combinations of the field operators of vacuum modes that are orthogonal to the mode \hat{s}_0 (for the proof, see Appendix A). Thus, in the measurement modes, any normally ordered average has the following property:

$$\langle : F(\hat{a}_m^\dagger, \hat{a}_n) : \rangle = \langle : F(A_m^* \hat{s}_0^\dagger, A_n \hat{s}_0) : \rangle, \quad (2)$$

where $: \hat{X} :$ denotes normal ordering, and F is an arbitrary analytical function of the field operators. Accordingly, the average number of detected photons in the m th measurement mode reads

$$N_m = \langle \hat{a}_m^\dagger \hat{a}_m \rangle = |A_m|^2 N_S. \quad (3)$$

Specifically for the scheme in Fig. 1, the coefficients:

$$A_m = \sqrt{\kappa} \int d\vec{r} f_m^*(\vec{r}) [u_0(\vec{r} - \vec{r}_1) \cos \theta + u_0(\vec{r} - \vec{r}_2) \exp(i\phi) \sin \theta], \quad (4)$$

depend on the source positions $\vec{r}_{1,2}$, their intensity asymmetry (as given by θ) and mutual phase ϕ , the transmissivity κ and the PSF $u_0(\vec{r})$ of the imaging system, and the shapes of the measurement modes $f_m(\vec{r})$.

III. MOMENT-BASED SENSITIVITY

To estimate the resolution of the considered optical scheme, we calculate the moment-based sensitivity (henceforth, we will refer to it simply as *sensitivity*). Within the framework of the method of moments, the error in the estimation of a set of parameters $\{q_\alpha\}$ from the optimal linear combinations $\{Y_\alpha\}$ of the mean values $\{X_m\}$ of commuting observables $\{\hat{X}_m\}$ is related to the sensitivity matrix [17]:

$$M_{\alpha\beta} = \sum_{m,n} (\Gamma^{-1})_{mn} \frac{\partial X_m}{\partial q_\alpha} \frac{\partial X_n}{\partial q_\beta}, \quad (5)$$

where $\Gamma_{mn} = \langle \hat{X}_m \hat{X}_n \rangle - X_m X_n$ is the covariance matrix of the observables. The inverse sensitivity matrix gives covariances for the estimators:

$$\text{cov}(\tilde{q}_\alpha, \tilde{q}_\beta) = \frac{1}{\mu} (M^{-1})_{\alpha\beta}, \quad (6)$$

where μ is the number of measurement repetitions (assumed to be large), and \tilde{q}_α are the unbiased estimators based on Y_α . This approach significantly simplifies measurement results processing and allows us to avoid inferring parameters from the full photon counting statistics, e.g., maximum likelihood estimation.

Generally, estimators that include all moments of the observables $\{\hat{X}_m\}$ can have lower variances, i.e., the following chain of inequalities holds [17]:

$$\mathbf{M}(\{q_\alpha\}, \{\hat{X}_m\}) \leq \mathcal{F}(\{q_\alpha\}, \{\hat{X}_m\}) \leq \mathcal{F}_Q(\{q_\alpha\}), \quad (7)$$

where $\mathbf{M}(\{q_\alpha\}, \{\hat{X}_m\})$ is the sensitivity matrix in Eq. (5), $\mathcal{F}(\{q_\alpha\}, \{\hat{X}_m\})$ is the FI matrix, $\mathcal{F}_Q(\{q_\alpha\})$ is the QFI matrix [29], and the matrix inequality $\mathbf{A} \leq \mathbf{B}$ means that $\vec{a}^T \mathbf{A} \vec{a} \leq \vec{a}^T \mathbf{B} \vec{a}$ for any given column vector \vec{a} . Thus, the sensitivity can be considered a lower bound for the FI. It was shown that the sensitivity of photon counting in Hermite-Gauss (HG) modes saturates the QFI for the estimation of the separation between equally bright uncorrelated thermal sources [8].

Using the expression in Eq. (5), one can calculate the sensitivity of photon counting in spatial modes $f_m(\vec{r})$, i.e., use $\hat{X}_m = \hat{a}_m^\dagger \hat{a}_m$ as observables. Thus, using the property in Eq. (2) and Eq. (3), one can find the elements of the photon number covariance matrix:

$$\Gamma_{mn} = \delta_{mn} N_m + h N_m N_n, \quad (8)$$

where $h = (\Delta N_S^2 - N_S)/N_S^2 = g^{(2)} - 1$, with $g^{(2)}$ the degree of second-order coherence. The matrix in Eq. (8) can be analytically inverted with the Sherman-Morrison formula [30], obtaining

$$(\Gamma^{-1})_{mn} = \delta_{mn} N_m^{-1} - \frac{h}{1 + h N_D}, \quad (9)$$

where $N_D = \sum_m N_m$ is the total number of detected photons. Then the sensitivity matrix in Eq. (5) can be expressed as

$$M_{\alpha\beta} = N_D \sum_m \frac{1}{\varepsilon_m} \frac{\partial \varepsilon_m}{\partial q_\alpha} \frac{\partial \varepsilon_m}{\partial q_\beta} + \frac{1}{\Delta N_D^2} \frac{\partial N_D}{\partial q_\alpha} \frac{\partial N_D}{\partial q_\beta}, \quad (10)$$

where $\varepsilon_m = N_m/N_D$ is the relative photon number, and

$$\Delta N_D^2 = \sum_{mn} \Gamma_{mn} = N_D(1 + h N_D) \quad (11)$$

is the variance of the total number of detected photons.

A. Single-parameter estimation

If all parameters except the separation d are known, the sensitivity matrix in Eq. (10) reduces to a single number:

$$M_d = N_D \sum_m \frac{1}{\varepsilon_m} \left(\frac{\partial \varepsilon_m}{\partial d} \right)^2 + \frac{1}{\Delta N_D^2} \left(\frac{\partial N_D}{\partial d} \right)^2. \quad (12)$$

The inverse of this quantity gives the variance of the separation estimator \tilde{d} :

$$\Delta \tilde{d}^2 = \frac{1}{\mu} (M_d)^{-1} = \frac{1}{\mu} \frac{1}{N_D M_\varepsilon + M_D}. \quad (13)$$

The expression in Eq. (12) has two terms. The first term equals $N_D M_\varepsilon$, where

$$M_\varepsilon = \sum_m \frac{1}{\varepsilon_m} \left(\frac{\partial \varepsilon_m}{\partial d} \right)^2 \quad (14)$$

does not depend on the state $\hat{\rho}_0$ of the principle mode (that does not mean that it is independent of the state of the sources which is also determined by θ and ϕ) but strongly depends on the measurement basis $\{f_m(\vec{r})\}$. Here, M_ε can be called the sensitivity per detected photon of relative intensity measurements. In the limit of small photon numbers where only a single photon is detected in the image plane, the probability of finding it in the m th mode equals ε_m . Thus, in this limit, M_ε coincides with the FI of postselected single-photon detection outcomes.

The second term:

$$M_D = \frac{1}{\Delta N_D^2} \left(\frac{\partial N_D}{\partial d} \right)^2, \quad (15)$$

does not depend on the individual signals N_m but only on the total number of detected photons N_D ; thus, it stays the same for any measurement basis $\{f_m(\vec{r})\}$ if all photons in the image

plane are detected. This additional sensitivity M_D occurs due to the interference of mutually coherent sources and the subsequent dependence of the total number of registered photons N_D on the separation d . The variance of the total number of detected photons in Eq. (11) depends on the quantum statistics of the source and grows with source bunching.

The expression in Eq. (15) has a self-consistent structure representing the simple error-propagation formula. In the small photon number limit, it equals the FI of measuring N_D ; thus, in this limit, the sensitivity in Eq. (12) fully coincides with the FI. In the next subsection, we show that the sensitivity M_D , coming from the total number of detected photons, vanishes if the brightness of the sources N_S is unknown.

B. Two-parameter estimation

To better understand the physical meaning of the quantities M_ε and M_D , let us consider the two-parameter problem, where both the separation d and the emitted number of photons N_S are unknown and treated as parameters to be estimated. The sensitivity matrix in Eq. (10) for the estimation of the parameters $q_\alpha = \{d, N_S\}$ reads

$$M_{\alpha\beta} = \begin{bmatrix} N_D M_\varepsilon + M_D & \frac{1}{\Delta N_D^2} \frac{\partial N_D}{\partial N_S} \frac{\partial N_D}{\partial d} \\ \frac{1}{\Delta N_D^2} \frac{\partial N_D}{\partial N_S} \frac{\partial N_D}{\partial d} & \frac{1}{\Delta N_D^2} \left(\frac{\partial N_D}{\partial N_S} \right)^2 \end{bmatrix}, \quad (16)$$

where $\partial \varepsilon_m / \partial N_S = 0$ is considered. In this case, the variance of the separation estimator \tilde{d} is given by

$$\Delta \tilde{d}^2 = \frac{1}{\mu} (M^{-1})_{11} = \frac{1}{\mu} \frac{1}{N_D M_\varepsilon}. \quad (17)$$

This formula shows that, without knowing the number of emitted photons N_S , one can benefit only from measurements of relative intensities ε_m . Comparing it with Eq. (13), one can see that knowing the number of emitted photons N_S increases the sensitivity of separation estimation by the sensitivity M_D obtained from the total detected number of photons. This fact fits well with the conclusions of the discussion about the effect of the partial coherence of thermal sources on the resolution [19,23]. From Eq. (17), one can conclude that ignorance of the brightness of the sources N_S wipes out any possible advantage from nonclassical statistics of the sources that are only present in the term M_D .

If one uses bucket detection which corresponds to the detection of all the photons in the image plane and can be described in this particular case as a single mode measurement in the principal mode, then the only relative intensity $\varepsilon_0 = 1$ does not depend on the parameter; thus, $M_\varepsilon = 0$. One cannot estimate separation from this measurement without knowing the number of emitted photons N_S . If N_S is known, then as expected, full sensitivity of bucket detection is provided by total photon number detection $M_d = M_D$.

Note that following the standard metrological approach, the position of the centroid $(\vec{r}_1 + \vec{r}_2)/2$ and the orientation of the pair of sources are assumed to be known prior to the measurement. Often these parameters, if unknown, can be estimated with an additional preparatory measurement. However, one should keep in mind that such an estimation has a finite precision, and for an asymmetric source, it is correlated with the estimation of the separation itself [31].

Moreover, we remark that, even though the structure of the sensitivity expression in Eq. (10) is quite intuitive, it was derived specifically for the single-mode (fully coherent) case and does not necessarily hold for other cases. For example, the estimation sensitivity for the separation of incoherent thermal sources depends nonlinearly on the brightness of the sources [8], although the total number of detected photons does not depend on the separation in this case.

It is worth mentioning that the used property in Eq. (2) is valid for a quite general class of parameter estimation schemes, where the parameters are encoded in an arbitrary number of mutually coherent modes, which are subjected to correlated parameter-dependent linear losses. Therefore, the formula in Eq. (10) for the sensitivity matrix of photon counting is valid for this wider class of systems since the explicit form of coefficients A_m in Eq. (4) was never used. Thus, the developed approach can be used for other problems, like coherent imaging [27] or quantum sensing in a continuous-variable entangled network in the single-mode regime [28].

IV. SENSITIVITY OF RELATIVE INTENSITY MEASUREMENTS M_ε

Now let us separately consider the two parts of the separation estimation sensitivity in Eq. (12). The sensitivity of the relative intensity measurement M_ε does not depend on the quantum state $\hat{\rho}_0$ but strongly depends on the measurement basis $\{f_m(\vec{r})\}$. As we already mentioned, it equals zero for bucket detection in the principal mode. Here, we consider two more measurement bases.

A. Direct imaging

By DI, we mean the measurement of the intensity distribution in the image plane. This distribution reads

$$I(\vec{r}) = \kappa N_S \left[u_0^2(\vec{r} - \vec{r}_1) \cos^2 \theta + u_0^2(\vec{r} - \vec{r}_2) \sin^2 \theta + u_0(\vec{r} - \vec{r}_1) u_0(\vec{r} - \vec{r}_2) \sin 2\theta \cos \phi \right], \quad (18)$$

where the PSF $u_0(\vec{r})$ is assumed to be real. Then the sensitivity of a relative intensity measurement in the continuous limit can be calculated as

$$M_\varepsilon^{\text{DI}} = \int \frac{1}{i(\vec{r})} \left[\frac{\partial i(\vec{r})}{\partial d} \right]^2 d\vec{r}, \quad (19)$$

with $i(\vec{r}) = I(\vec{r})/N_D$, where the total number of detected photons is given by

$$N_D = \int I(\vec{r}) d\vec{r} = \kappa N_S (1 + \chi \delta). \quad (20)$$

In turn, we introduced the parameters:

$$\chi = \sin 2\theta \cos \phi, \quad (21)$$

being the amplitude of the interference term in Eq. (18), and δ is the overlap between the images of the sources:

$$\delta = \int u_0(\vec{r} - \vec{r}_1) u_0(\vec{r} - \vec{r}_2) d\vec{r}. \quad (22)$$

The expression in Eq. (20) is valid for any measurement basis in which one can decompose the image mode. Hereinafter, we

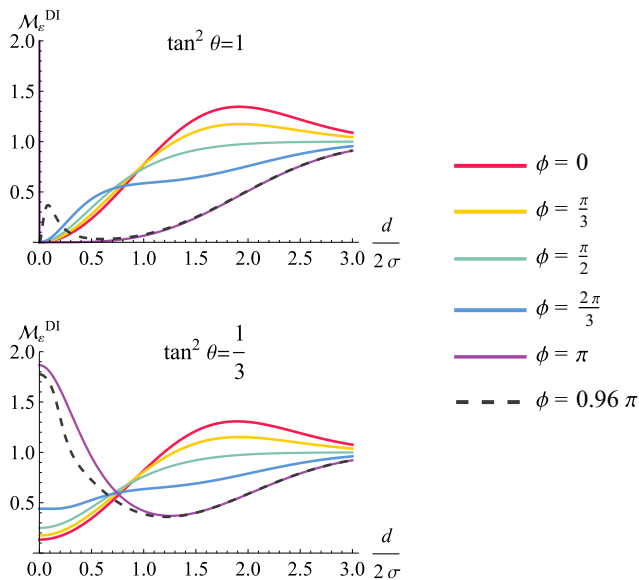


FIG. 2. Normalized sensitivity per emitted photon of relative intensity distribution direct measurement $\mathcal{M}_\varepsilon^{\text{DI}}$. The top panel corresponds to the sources with equal intensity and parameter $\chi = \{1, 1/2, 0, -1/2, -1, -0.99\}$; the bottom panel shows the asymmetric case and $\chi = \{0.87, 0.43, 0, -0.43, -0.87, -0.86\}$.

consider a soft aperture model with a Gaussian PSF:

$$u_0(\vec{r}) = \sqrt{\frac{1}{2\pi\sigma^2}} \exp\left(-\frac{|\vec{r}|^2}{4\sigma^2}\right), \quad (23)$$

where σ is the width of the PSF. This results in an overlap:

$$\delta = \exp\left(-\frac{d^2}{8\sigma^2}\right). \quad (24)$$

The sensitivity in Eq. (19) can be calculated analytically in the cases of in-phase ($\phi = 0$) and antiphase ($\phi = \pi$) sources:

$$\mathcal{M}_\varepsilon^{\text{DI}}|_{\phi=0,\pi} = \frac{1}{4\sigma^2(1+\chi\delta)} \left(1 - \chi\delta + \frac{d^2}{4\sigma^2} \frac{\chi\delta}{1+\chi\delta}\right), \quad (25)$$

and in the case of fully asymmetric sources ($\theta = 0$, which is equivalent to the centroid estimation of a single source), giving the well known result [4,32]:

$$\mathcal{M}_\varepsilon^{\text{DI}}|_{\theta=0} = \frac{1}{4\sigma^2}. \quad (26)$$

For other values of ϕ and θ , the sensitivity $\mathcal{M}_\varepsilon^{\text{DI}}$ is calculated numerically.

The variable M_ε corresponds to the sensitivity per detected photon. The sensitivity per emitted photon is instead given by $N_D M_\varepsilon / N_S$. We additionally normalize this value over transmissivity κ and multiply by $4\sigma^2$ to remove dependence on these parameters. A plot of the resulting normalized sensitivity:

$$\mathcal{M}_\varepsilon = \frac{4\sigma^2 N_D M_\varepsilon}{\kappa N_S}, \quad (27)$$

for the case of DI, is presented in Fig. 2.

On the top panel of Fig. 2, one can see that direct measurement of the relative intensity distribution in the case of equally

bright sources leads to low sensitivity for small separations and, as expected, to Raleigh's curse, i.e., vanishingly small sensitivity for infinitesimally small d . In the case of asymmetric sources, the first moment of the intensity distribution, i.e., the center of mass of the image, does not coincide with the geometrical center between sources. Assuming the position of the geometrical center between the sources and the brightness of both sources to be known, one can recover the separation between the sources from the center of mass of the image, which can be accurately measured with DI. Accordingly, Raleigh's curse does not occur for DI of asymmetric sources (bottom of Fig. 2), although the sensitivity is relatively small for small separation, unless the sources are nearly in antiphase configuration.

B. Spatial-mode demultiplexing

Another imaging technique under study is SPADE. It was shown that the sensitivity of photon counting in HG modes saturates the QFI for the estimation of the separation between two equally bright incoherent thermal sources in the case of a Gaussian PSF [8]. This measurement also beats DI in the asymmetric case (unequally bright sources), though the optimality of the HG basis was never proved for this case.

Here, we analyze the sensitivity of photon counting in HG modes in the case of fully coherent bright sources in an arbitrary quantum state. As before, we assume to know all the source parameters except the separation [in Eqs. (12) and (16)] and the total brightness N_S [only in Eq. (16)]. Thus, the reference system and the measurement basis can be chosen aligned with the image centroid and orientation, i.e., the measurement HG mode basis reads

$$f_m(x, y) = \frac{1}{\sqrt{2^m m!}} H_m\left(\frac{x}{\sqrt{2}\sigma}\right) u_0(\sqrt{x^2 + y^2}), \quad (28)$$

where H_m are Hermite polynomials, and the source positions read $\vec{r}_{1,2} = \{\pm d/2, 0\}$. Calculating the overlaps with the image modes, we find that the coefficients A_m in Eq. (4) are given by

$$A_m^{\text{HG}} = \sqrt{\kappa} [(-1)^m \cos\theta + \exp(i\phi) \sin\theta] \beta_m\left(\frac{d}{4\sigma}\right), \quad (29)$$

where

$$\beta_m(x) = \exp\left(-\frac{x^2}{2}\right) \frac{x^m}{\sqrt{m!}}. \quad (30)$$

This allows us to find the mean photon numbers in the measurement modes in Eq. (3):

$$N_m^{\text{HG}} = N_S [1 + (-1)^m \chi] \beta_m^2\left(\frac{d}{4\sigma}\right). \quad (31)$$

These can be normalized with respect to the total number of detected photons N_D in Eq. (20) to calculate the sensitivity in Eq. (14) of the separation estimation from the measured relative photon numbers ε_m . In the case of infinitely many measured HG modes, this sensitivity reads

$$\mathcal{M}_\varepsilon^{\text{HG}} = \frac{1}{4\sigma^2(1+\chi\delta)} \left(1 - \chi\delta + \frac{d^2}{4\sigma^2} \frac{\chi\delta}{1+\chi\delta}\right). \quad (32)$$

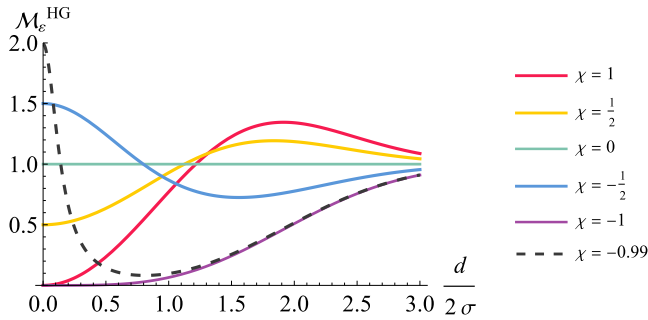


FIG. 3. Normalized sensitivity per emitted photon of relative intensity measurements in Hermite-Gauss (HG) modes $\mathcal{M}_\epsilon^{\text{HG}}$.

Note that $\mathcal{M}_\epsilon^{\text{HG}}$ depends only on the combination χ of the parameters θ and ϕ .

We observe that the expression for the sensitivity of SPADE $\mathcal{M}_\epsilon^{\text{HG}}$ in Eq. (32) coincides with the sensitivity of DI $\mathcal{M}_\epsilon^{\text{DI}}$ in the cases of in-phase, antiphase in Eq. (25), and fully asymmetric sources in Eq. (26). It is possible to show that these are the only cases for which $\mathcal{M}_\epsilon^{\text{HG}} = \mathcal{M}_\epsilon^{\text{DI}}$. In the general case (see Appendix B),

$$\mathcal{M}_\epsilon^{\text{HG}} \geq \mathcal{M}_\epsilon^{\text{DI}}. \quad (33)$$

Accordingly, measurements in the HG basis are always more (or equally) sensitive than DI for separation estimation.

In Fig. 3, we plot the normalized sensitivity in Eq. (27) of the relative intensity measurement in the HG modes. One can see that Raleigh's curse is still present for the symmetric in-phase ($\chi = 1$) and antiphase ($\chi = -1$) cases since SPADE for these cases is as sensitive as DI. Note, however, that even a small deviation from the symmetric antiphase case ($\chi = -1$) leads to a significant sensitivity increase for small separations (see dashed line in Fig. 3).

The sensitivity in Eq. (32) in the case $\chi = 0$ (that corresponds to the mutual phase $\phi = \pi/2$) does not depend on the separation d and coincides with the sensitivity in the case of weak uncorrelated thermal sources [9], which in turn coincides with QFI [15]. However, for incoherent thermal sources, the QFI per emitted photon drops with a growing number of photons, when $\mathcal{M}_\epsilon^{\text{HG}}$ for correlated sources does not depend on N_S for any photon statistics of the source.

V. SENSITIVITY OF TOTAL INTENSITY MEASUREMENT M_D

Having an expression for the total number of detected photons in Eq. (20), we analytically determine the total photon number sensitivity in Eq. (15):

$$M_D = \frac{\kappa N_S}{4\sigma^2} \frac{\delta^2 \chi^2}{(1 + \delta\chi) + h\kappa N_S(1 + \delta\chi)^2} \left(\frac{d}{2\sigma}\right)^2. \quad (34)$$

Since the total intensity is basis invariant, the sensitivity from measuring it does not depend on the detection basis. The expression in Eq. (34) also includes all quantum states of the sources (if the sources are mutually coherent) via the coefficient $h = g^{(2)} - 1 = (\Delta N_S^2 - N_S)/N_S^2$. From Eq. (34), it

is obvious that antibunched states of \hat{s}_0 ($h < 0$), leading to entanglement in modes $\hat{s}_{1,2}$, provide a better sensitivity than bunched states ($h > 0$) of \hat{s}_0 , which corresponds to classical correlations in $\hat{s}_{1,2}$. This is a natural result since a lower photon number variance in \hat{s}_0 leads to a smaller variance of N_D and hence a higher sensitivity of the N_D measurement.

Here, we consider the sensitivity of separation estimation from a measured total intensity N_D for different quantum statistics of the sources. We are interested in the normalized sensitivity per emitted photon:

$$\mathcal{M}_D = \frac{4\sigma^2}{\kappa} \frac{M_D}{N_S}. \quad (35)$$

The characteristics of the source statistics only appear in the combination $h\kappa N_S$. Furthermore, \mathcal{M}_D depends on χ and the separation d . To explore the impact of the source statistics, we study various common initial states.

A. Fock state

We consider first the most sensitive case, when the mode \hat{s}_0 is maximally antibunched, i.e., it is in the Fock state, resulting in the entanglement of the modes $\hat{s}_{1,2}$. In this case, $h = g^{(2)} - 1 = -1/N_S$, and the combination $h\kappa N_S = -\kappa$. On the left panel of Fig. 4, we plot the sensitivity \mathcal{M}_D in Eq. (35) with $\kappa = 0.2$ (the used model of linear losses requires $\kappa \ll 1$). Note that, for the Fock state, the sensitivity per emitted photon does not depend on the number of photons N_S .

B. Coherent state

If the mode \hat{s}_0 is in the coherent state, then the states of the modes $\hat{s}_{1,2}$ are uncorrelated. For this case, the parameter $h = 0$. Although coherent and Fock states have very different statistical properties, in both cases, after propagation through a loss channel, the photon number variance is linear over the initial number of photons; thus, the sensitivity per emitted photon does not depend on the source intensity for both of these cases. The normalized sensitivity for the case of a coherent source is plotted in the middle panel of Fig. 4.

C. Thermal state

Finally, we consider a thermal state of the mode \hat{s}_0 , which leads to correlated thermal states in modes $\hat{s}_{1,2}$. For thermal statistics, $h = 1$. In the small photon number limit ($N_S \rightarrow 0$), the sensitivity per emitted photon \mathcal{M}_D coincides with the coherent case, and for high photon number ($N_S \rightarrow \infty$), it vanishes ($\mathcal{M}_D \rightarrow 0$). We plot the normalized total photon-number sensitivity for correlated thermal sources for $\kappa N_S = 1.5$ in the right panel of Fig. 4.

For all the considered cases, the total photon-number sensitivity is high in the case of small separation between symmetric antiphase sources ($\chi = -1$). This occurs due to destructive interference of mutually coherent antiphase sources, which leads to zero intensity in the image plane if equally bright sources coincide and nonzero total intensity in the presence of finite separation between the sources. For any other case, the sensitivity M_D vanishes for zero separation. In

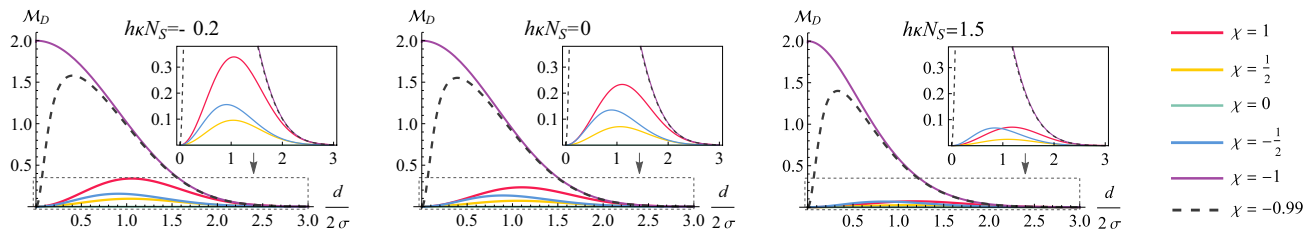


FIG. 4. Normalized sensitivity of total photon number detection \mathcal{M}_D . From left to right: Fock ($\kappa = 0.2$), coherent and thermal state ($N_S = 1.5/\kappa$) of the mode \hat{s}_0 .

the case of $\chi = 0$, the total photon number N_D in Eq. (20) does not depend on the parameter, and $M_D = 0$.

VI. COMPARISON WITH QFI

Here, we analyze the full separation estimation sensitivity $M_d = N_D M_\varepsilon + M_D$ and its normalized version:

$$\mathcal{M}_d = \frac{4\sigma^2}{\kappa} \frac{M_d}{N_S} = \mathcal{M}_\varepsilon + \mathcal{M}_D. \quad (36)$$

We compare the sensitivity of SPADE, which proved to always be better or equal to that of DI, with the ultimate limit set by the QFI.

A. Fock state

The first example we consider is a Fock state of the mode \hat{s}_0 . Plots of the SPADE sensitivity for split Fock states are presented in the left panel of Fig. 5.

Of particular interest are the examples of the Fock state split on a symmetric beam splitter ($\theta = \pi/4$) with added phase $\phi = 0$ or π . Then the states of the sources take the form:

$$|\psi\rangle_{s_1 s_2}^{(\pm)} = \frac{1}{\sqrt{2^{N_S}}} \sum_{j=0}^{N_S} \sqrt{\binom{N_S}{j}} (\pm 1)^{N_S-j} |j\rangle_{s_1} |N_S - j\rangle_{s_2}. \quad (37)$$

The analytical expression obtained for the SPADE sensitivity M_d^{HG} coincides with the QFI for these states [15]. Note that one of these states corresponds to the maximal QFI of separation estimation [as seen from Fig. 5, for small separations, state $|\psi\rangle_{s_1 s_2}^{(-)}$ is optimal, for larger, $|\psi\rangle_{s_1 s_2}^{(+)}$] [15]. For other

values of the mutual phase ϕ or asymmetrically split Fock states, the QFI has not been calculated explicitly.

B. Coherent state

Since for Poisson photon number statistics different detection events are independent, we can consider results in the small photon number limit without losing any generality. The QFI for an arbitrary mutual coherence γ was explicitly calculated in Ref. [23] in the single-photon subspace, and its analytical expression for any $\gamma = \exp(i\phi)$ fully coincides with the sensitivity M_d calculated for Poisson statistics ($h = 0$). The same result was recently obtained for arbitrarily bright coherent sources in Ref. [26]. The dependence of the normalized QFI and $\mathcal{M}_d^{\text{HG}}$ on the separation are presented in the middle panel of Fig. 5, coinciding with each other.

We also plot the sensitivity of DI for symmetric sources with Poisson statistics in Fig. 6. Comparing this plot to the middle panel of Fig. 5, we clearly see that the choice of HG modes (SPADE) results in a significant advantage over pixel modes (DI). The special case of symmetric antiphase sources ($\chi = -1$) leads to the collapse of the DI sensitivity and to Raleigh's curse once mutual phase slightly deviates from π .

C. Thermal state

Another example we consider is that of correlated thermal sources. The QFI for arbitrarily bright correlated thermal sources that are in-phase or antiphase is calculated in Ref. [15]. A more general case with arbitrary Gaussian sources is considered in Ref. [26]. The QFI obtained in these papers for equally bright sources coincides with the sensitivity

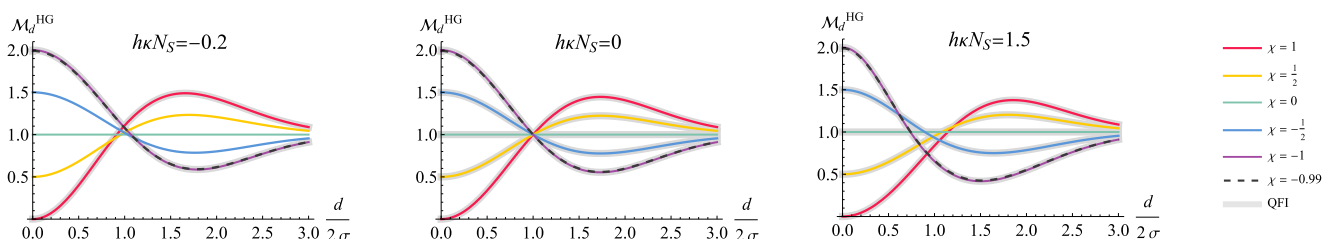


FIG. 5. Normalized full separation estimation sensitivity $\mathcal{M}_d^{\text{HG}}$ via spatial-mode demultiplexing (SPADE) in Hermite-Gauss (HG) basis. From left to right: Fock ($\kappa = 0.2$), coherent and thermal state ($N_S = 1.5/\kappa$) of the mode \hat{s}_0 . Cases with known quantum Fisher information (QFI) are highlighted in gray; QFI and M_d^{HG} coincide for all of them.

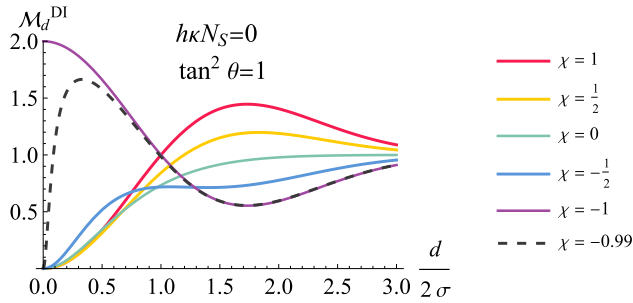


FIG. 6. Normalized full separation estimation sensitivity of direct imaging (DI) $\mathcal{M}_d^{\text{DI}}$ for equally bright sources with Poisson statistics.

$\mathcal{M}_d^{\text{HG}}$ introduced here. With increasing intensity of the correlated thermal source, the sensitivity per photon \mathcal{M}_d drops tending to \mathcal{M}_ε (Fig. 3).

Figure 5 shows that source statistics do not strongly influence the sensitivity if the sources are mutually coherent. We notice that the resulting sensitivity of SPADE $\mathcal{M}_d^{\text{HG}}$ is continuous as a function of χ , which is not the case for DI.

VII. CONCLUSIONS

We presented a general approach to analyze parameter estimation problems based on photon counting in mutually coherent modes. The sensitivity based on the method of moments showed to be a very efficient and practical tool for analyzing this class of problems. In contrast to the traditional approach based on FI, moment-based sensitivity allows us to consider the sources with arbitrary quantum statistics and provide a simple estimator for the parameters that does not require measurement of high-order moments.

Specifically, we have considered in detail the problem of separation estimation of two mutually coherent sources. Calculating the moment-based sensitivity, we analytically proved an advantage of SPADE measurement over DI for the considered class of states. Moreover, we showed that the sensitivity of SPADE saturates the QFI for those cases where the latter is known. This even includes some examples of non-Gaussian entangled states, although they are not fully described by the first two moments, which we used to compute the sensitivity.

We showed that the sensitivity consists of two terms that correspond to the relative photon numbers in the detected modes and to the total number of detected photons, respectively. The first term only depends on the measurement basis, while the second one depends on quantum statistics of the sources. Moreover, the second term vanishes in case of unknown brightness of the sources, wiping out any advantage from the antibunching of the sources. The sensitivity from the total photon number measurement is also negligible for intense bunched states due to the high noise in the total number of photons.

Finally, the moment-based sensitivity approach and the results obtained in this paper can be applied to other parameter estimation problems with mutually coherent or single-mode sources, like coherent imaging or distributed quantum sensing with mutually coherent probes.

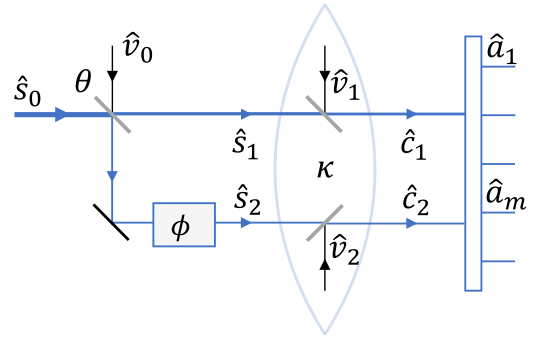


FIG. 7. Conceptual scheme for describing evolution of the field in the imaging system.

ACKNOWLEDGMENTS

I.K. acknowledges support from the PAUSE National programme. This paper received funding from Ministerio de Ciencia e Innovación (MCIN)/Agencia Estatal de Investigación (AEI) for Project No. PID2020-115761RJ-I00 and support of a fellowship from “la Caixa” Foundation (ID 100010434) and from the European Union’s Horizon 2020 research and innovation program under Marie Skłodowska-Curie Grant Agreement No. 847648, fellowship code LCF/BQ/PI21/11830025. This paper was partially funded by CEX2019-000910-S [MCIN/AEI/10.13039/501100011033], Fundació Cellex, Fundació Mir-Puig, and Generalitat de Catalunya through CERCA. This paper was partially funded by French ANR under the COSMIC project (ANR-19-ASTR-0020-01). This paper received funding from the European Union’s Horizon 2020 research and innovation programme under Grant Agreement No. 899587. This paper was supported by the European Union’s Horizon 2020 research and innovation programme under the QuantERA programme through the project ApresSF. M.G. acknowledges funding by the Generalitat Valenciana (CDEIGENT/2021/014).

APPENDIX A: FIELD EVOLUTION

To connect the field operators of the measurement modes \hat{a}_m and the field operator of the principal mode \hat{s}_0 , one can represent light transformation in the imaging scheme as in Fig. 7. Due to the finite size of the imaging system, part of the light emitted by the sources is lost to the environment. These losses can be described as mixing light with environmental vacuum modes $\hat{v}_{1,2}$ [8,15]. Since both sources are losing light to a common environment, modes $\hat{v}_{1,2}$ are mutually nonorthogonal.

The beam splitter θ and the phase element ϕ describe the transition from principal mode \hat{s}_0 to the modes of the sources $\hat{s}_{1,2}$. Assuming the beam splitter to introduce no additional phase to the modes, this transformation takes form:

$$\begin{pmatrix} \hat{s}_1 \\ \hat{s}_2 \end{pmatrix} = \begin{bmatrix} 1 & 0 \\ 0 & \exp(i\phi) \end{bmatrix} \begin{pmatrix} \cos \theta & -\sin \theta \\ \sin \theta & \cos \theta \end{pmatrix} \begin{pmatrix} \hat{s}_0 \\ \hat{v}_0 \end{pmatrix}, \quad (\text{A1})$$

where \hat{v}_0 is the field operator of a vacuum mode.

The considered imaging system performs linear transformation of the field, i.e., the field operators \hat{a}_m of the

measurement modes $f_m(\vec{r})$ can be expressed as

$$\hat{a}_m = x_m^{(1)} \hat{s}_1 + x_m^{(2)} \hat{s}_2 + \hat{v}'_m, \quad (\text{A2})$$

where $x_m^{(1,2)}$ are complex coefficients, and \hat{v}'_m are nonnormalized combinations of the field operators of vacuum modes.

We find coefficients $x_m^{(1)}$ by considering situations where mode \hat{s}_2 is in the vacuum state. For this, we represent linear losses on the finite aperture of the imaging system as mixing mode \hat{s}_1 with the vacuum mode \hat{v}_1 [15]. Then the state of the field in the detection plane is fully described by the single mode $u_0(\vec{r} - \vec{r}_1)$ (called the *image mode*) with the field operator:

$$\hat{c}_1 = \sqrt{\kappa} \hat{s}_1 + \sqrt{1 - \kappa} \hat{v}_1, \quad (\text{A3})$$

with κ being system transmissivity. Mode $u_0(\vec{r} - \vec{r}_1)$ can be decomposed over the orthogonal set of measurement modes $\{f_m(\vec{r})\}$; thus, the field operators of the measurement modes in case of a single light source \hat{s}_1 is represented as

$$\hat{a}_m^{(1)} = \left[\int f_m^*(\vec{r}) u_0(\vec{r} - \vec{r}_1) d\vec{r} \right] \hat{c}_1 + \hat{v}_m^{(1)}. \quad (\text{A4})$$

Substituting here Eq. (A3) and comparing the result with Eq. (A2), we arrive at

$$x_m^{(1)} = \sqrt{\kappa} \int f_m^*(\vec{r}) u_0(\vec{r} - \vec{r}_1) d\vec{r}. \quad (\text{A5})$$

In a similar way, we find coefficients $x_m^{(2)}$ by considering mode \hat{s}_1 being in a vacuum state, obtaining the final result:

$$\hat{a}_m = \sqrt{\kappa} \sum_j \left[\int f_m^*(\vec{r}) u_0(\vec{r} - \vec{r}_j) d\vec{r} \right] \hat{s}_j + \hat{v}'_m. \quad (\text{A6})$$

Then using Eq. (A1), we arrive at

$$\hat{a}_m = A_m \hat{s}_0 + \hat{v}_m, \quad (\text{A7})$$

where \hat{v}_m are nonnormalized nonorthogonal combinations of the field operators of vacuum modes, and

$$A_m = \sqrt{\kappa} \int d\vec{r} f_m^*(\vec{r}) [u_0(\vec{r} - \vec{r}_1) \cos \theta + u_0(\vec{r} - \vec{r}_2) \exp(i\phi) \sin \theta]. \quad (\text{A8})$$

APPENDIX B: PROOF OF SPADE ADVANTAGE OVER DI

Theorem.

$$\Delta M = M_d^{\text{HG}} - M_d^{\text{DI}} \geq 0, \quad (\text{B1})$$

i.e., separation estimation sensitivity with SPADE measurements in the HG basis outperforms DI for any pair of mutually coherent sources. The inequality in Eq. (B1) is saturated only in cases $\phi = 0$, $\phi = \pi$, or $\theta = 0$.

Proof. To estimate the difference in Eq. (B1), one can rewrite the sensitivity in the following way:

$$M_d = \sum_m \frac{1}{N_m} \left(\frac{\partial N_m}{\partial d} \right)^2 - \frac{h}{1 + hN_D} \left(\frac{\partial N_D}{\partial d} \right)^2, \quad (\text{B2})$$

where the second term is independent of the measurement basis. Then

$$\Delta M = M_0^{\text{HG}}(\theta, \phi) - M_0^{\text{DI}}(\theta, \phi), \quad (\text{B3})$$

where

$$M_0(\theta, \phi) = \sum_m \frac{1}{N_m} \left(\frac{\partial N_m}{\partial d} \right)^2. \quad (\text{B4})$$

From the equality $M_\varepsilon^{\text{DI}}|_{\phi=0} = M_\varepsilon^{\text{HG}}|_{\phi=0}$, it follows that

$$M_0^{\text{DI}}(\theta, 0) = M_0^{\text{HG}}(\theta, 0) \quad (\text{B5})$$

since the difference between M_ε and M_0 is basis independent. At the same time, M_0^{HG} depends only on the parameter combination $\chi = \sin 2\theta \cos \phi$. Then for any $\phi \leq \pi/2$, one can use the following chain of equalities:

$$M_0^{\text{HG}}(\theta, \phi) = M_0^{\text{HG}}(\theta_1, 0) = M_0^{\text{DI}}(\theta_1, 0), \quad (\text{B6})$$

where $\sin 2\theta_1 = \sin 2\theta \cos \phi$. One can redo all the following analysis for $\phi \geq \pi/2$ using the fact that $M_\varepsilon^{\text{DI}}|_{\phi=\pi} = M_\varepsilon^{\text{HG}}|_{\phi=\pi}$; therefore, results are true for any value of ϕ .

Thus, the difference in sensitivity can be expressed as

$$\Delta M = M_0^{\text{DI}}(\theta_1, 0) - M_0^{\text{DI}}(\theta, \phi). \quad (\text{B7})$$

For continuous DI, the formula in Eq. (B4) takes the form:

$$M_0^{\text{DI}}(\theta, \phi) = \int \frac{1}{I_{\theta, \phi}(\vec{r})} \left[\frac{\partial I_{\theta, \phi}(\vec{r})}{\partial d} \right]^2 d\vec{r}, \quad (\text{B8})$$

where $I_{\theta, \phi}(\vec{r}) = |E_{\theta, \phi}(\vec{r})|^2$, and

$$E_{\theta, \phi}(\vec{r}) = u_0(\vec{r} - \vec{r}_1) \cos \theta + u_0(\vec{r} - \vec{r}_2) \exp(i\phi) \sin \theta. \quad (\text{B9})$$

A simple transformations leads to

$$\begin{aligned} M_0^{\text{DI}}(\theta, \phi) &= 2 \operatorname{Re} \left(\int \left\{ \frac{E_{\theta, \phi}^*(\vec{r})}{E_{\theta, \phi}(\vec{r})} [E'_{\theta, \phi}(\vec{r})]^2 + |E'_{\theta, \phi}(\vec{r})|^2 \right\} d\vec{r} \right), \end{aligned} \quad (\text{B10})$$

where $E'_{\theta, \phi}(\vec{r})$ stands for the derivative with respect to the separation d . Using the inequality:

$$\operatorname{Re} \left[\int g(x) dx \right] \leq \int |g(x)| dx, \quad (\text{B11})$$

for the first term in Eq. (B10), we find that

$$M_0^{\text{DI}}(\theta, \phi) \leq 4 \int |E'_{\theta, \phi}(\vec{r})|^2 d\vec{r}. \quad (\text{B12})$$

Since $E_{\theta_1, 0}(\vec{r}) \in \mathbb{R}$, then Eq. (B10) in this special case simplifies to

$$M_0^{\text{DI}}(\theta_1, 0) = 4 \int |E'_{\theta_1, 0}(\vec{r})|^2 d\vec{r}. \quad (\text{B13})$$

By using the explicit expression for the electric field in Eq. (B9), we can calculate the integral from the right part of Eq. (B12). The result depends only on $\chi = \sin 2\theta \cos \phi$. This means that the right parts of Eqs. (B12) and (B13) are equal, resulting in

$$\frac{\Delta M}{4} \geq \int |E'_{\theta_1, 0}(\vec{r})|^2 d\vec{r} - \int |E'_{\theta, \phi}(\vec{r})|^2 d\vec{r} = 0. \quad (\text{B14})$$

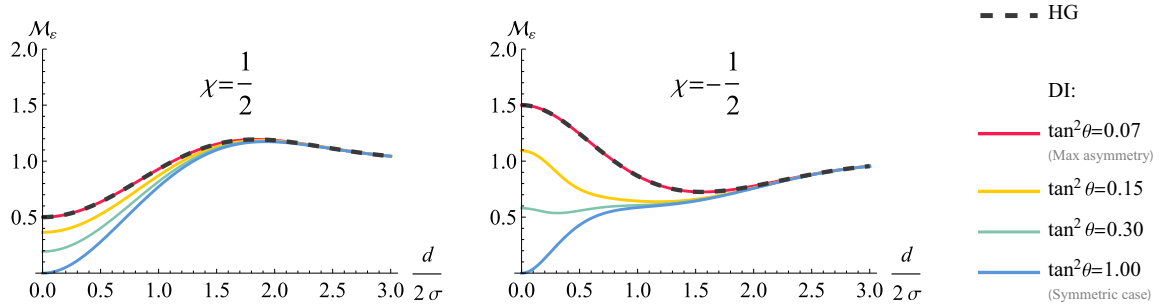


FIG. 8. Sensitivity per emitted photon of relative intensity measurement. Comparison of direct imaging (DI) with the spatial-mode demultiplexing (SPADE) technique.

The inequality in Eq. (B11) is only saturated if $g(x) = |g(x)|$, i.e.,

$$\frac{E_{\theta,\phi}^*(\vec{r})}{E_{\theta,\phi}(\vec{r})} [E'_{\theta,\phi}(\vec{r})]^2 = \left| \frac{E_{\theta,\phi}^*(\vec{r})}{E_{\theta,\phi}(\vec{r})} [E'_{\theta,\phi}(\vec{r})]^2 \right|, \quad (\text{B15})$$

for any \vec{r} . This equality holds only in cases $\phi = 0$, $\phi = \pi$, or $\theta = 0$.

In Fig. 8, you can find a comparison of the DI and SPADE sensitivities, built with fixed combinations $\chi = \sin 2\theta \cos \phi$ but with a different ratio between parameters ϕ and θ . These plots illustrate all given relations between M_d^{HG} and M_D^{DI} .

[1] L. Rayleigh, XXXI. Investigations in optics, with special reference to the spectrocope, *London, Edinburgh Dublin Philos. Mag. J. Sci.* **8**, 261 (1879).

[2] C. M. Sparrow, On spectroscopic resolving power, *Astrophys. J.* **44**, 76 (1916).

[3] C. W. Helstrom, Image restoration by the method of least squares, *J. Opt. Soc. Am.* **57**, 297 (1967).

[4] M. Tsang, R. Nair, and X.-M. Lu, Quantum Theory of Super-resolution for Two Incoherent Optical Point Sources, *Phys. Rev. X* **6**, 031033 (2016).

[5] R. Nair and M. Tsang, Far-Field Superresolution of Thermal Electromagnetic Sources at the Quantum Limit, *Phys. Rev. Lett.* **117**, 190801 (2016).

[6] M. Tsang, Resolving starlight: a quantum perspective, *Contemp. Phys.* **60**, 279 (2019).

[7] C. Datta, Y. L. Len, K. Łukanowski, K. Banaszek, and M. Jarzyna, Sub-rayleigh characterization of a binary source by spatially demultiplexed coherent detection, *Opt. Express* **29**, 35592 (2021).

[8] G. Sorelli, M. Gessner, M. Walschaers, and N. Treps, Moment-based superresolution: formalism and applications, *Phys. Rev. A* **104**, 033515 (2021).

[9] G. Sorelli, M. Gessner, M. Walschaers, and N. Treps, Optimal Observables and Estimators for Practical Superresolution Imaging, *Phys. Rev. Lett.* **127**, 123604 (2021).

[10] J. Shao and X.-M. Lu, Information regret tradeoff relation for locating two incoherent optical point sources *Phys. Rev. A* **105**, 062416 (2022).

[11] M. R. Grace, Z. Dutton, A. Ashok, and S. Guha, Approaching quantum-limited imaging resolution without prior knowledge of the object location, *J. Opt. Soc. Am. A* **37**, 1288 (2020).

[12] M. Paúr, B. Stoklasa, Z. Hradil, L. L. Sánchez-Soto, and J. Rehacek, Achieving the ultimate optical resolution, *Optica* **3**, 1144 (2016).

[13] F. Yang, A. Tashchilina, E. S. Moiseev, C. Simon, and A. I. Lvovsky, Far-field linear optical superresolution via heterodyne detection in a higher-order local oscillator mode, *Optica* **3**, 1148 (2016).

[14] P. Boucher, C. Fabre, G. Labroille, and N. Treps, Spatial optical mode demultiplexing as a practical tool for optimal transverse distance estimation, *Optica* **7**, 1621 (2020).

[15] C. Lupo and S. Pirandola, Ultimate Precision Bound of Quantum and Subwavelength Imaging, *Phys. Rev. Lett.* **117**, 190802 (2016).

[16] M. Gessner, A. Smerzi, and L. Pezzè, Metrological Nonlinear Squeezing Parameter, *Phys. Rev. Lett.* **122**, 090503 (2019).

[17] M. Gessner, A. Smerzi, and L. Pezzè, Multiparameter squeezing for optimal quantum enhancements in sensor networks, *Nat. Commun.* **11**, 3817 (2020).

[18] W. Larson and B. E. A. Saleh, Resurgence of Rayleigh’s curse in the presence of partial coherence, *Optica* **5**, 1382 (2018).

[19] M. Tsang and R. Nair, Resurgence of Rayleigh’s curse in the presence of partial coherence: comment, *Optica* **6**, 400 (2019).

[20] W. Larson and B. E. A. Saleh, Resurgence of Rayleigh’s curse in the presence of partial coherence: reply, *Optica* **6**, 402 (2019).

[21] Z. Hradil, J. Řeháček, L. Sánchez-Soto, and B.-G. Englert, Quantum Fisher information with coherence, *Optica* **6**, 1437 (2019).

[22] K. Liang, S. A. Wadood, and A. Vamivakas, Coherence effects on estimating two-point separation, *Optica* **8**, 243 (2021).

[23] S. Kurdzialek, Back to sources—the role of losses and coherence in super-resolution imaging revisited, *Quantum* **6**, 697 (2022).

[24] Z. Hradil, D. Koutný, and J. Řeháček, Exploring the ultimate limits: super-resolution enhanced by partial coherence, *Opt. Lett.* **46**, 1728 (2021).

[25] S. De, J. Gil-Lopez, B. Brecht, C. Silberhorn, L. L. Sánchez-Soto, Z. c. v. Hradil, and J. Řeháček, Effects of coherence on temporal resolution, *Phys. Rev. Res.* **3**, 033082 (2021).

[26] G. Sorelli, M. Gessner, M. Walschaers, and N. Treps, Gaussian quantum metrology for mode-encoded parameters: general theory and imaging applications, [arXiv:2202.10355](https://arxiv.org/abs/2202.10355).

- [27] P. Ferraro, A. Wax, and Z. Zalevsky, *Coherent Light Microscopy: Imaging and Quantitative Phase Analysis* (Springer-Verlag, Berlin, Heidelberg, 2011), Vol. 46.
- [28] X. Guo, C. R. Breum, J. Borregaard, S. Izumi, M. V. Larsen, T. Gehring, M. Christandl, J. S. Neergaard-Nielsen, and U. L. Andersen, Distributed quantum sensing in a continuous-variable entangled network, *Nat. Phys.* **16**, 281 (2020).
- [29] D. Petz and C. Ghinea, Introduction to quantum Fisher information, in *Quantum Probability and Related Topics* (World Scientific, Singapore, 2011), pp. 261–281.
- [30] J. Sherman and W. J. Morrison, Adjustment of an inverse matrix corresponding to a change in one element of a given matrix, *Ann. Math. Stat.* **21**, 124 (1950).
- [31] J. Řehaček, Z. Hradil, B. Stoklasa, M. Paúr, J. Grover, A. Krzic, and L. L. Sánchez-Soto, Multiparameter quantum metrology of incoherent point sources: towards realistic superresolution, *Phys. Rev. A* **96**, 062107 (2017).
- [32] C. Fabre, J. B. Fouet, and A. Maître, Quantum limits in the measurement of very small displacements in optical images, *Opt. Lett.* **25**, 76 (2000).